Models for electron transport

Journées SFPM

E. D'HUMIERES[2] B. DUBROCA[2] R. DUCLOUS[2] J.-L. FEUGEAS[2] F. FILBET[1] M. FRANK[3] J. MALLET[3] Ph. NICOLAI[2] C. REGAN[2]

[1]Université Lyon
[2]Université Bordeaux I
[3]TU Kaiserslautern

9 novembre 2010

Physics of the inertial fusion

Laser-driven inertial fusion

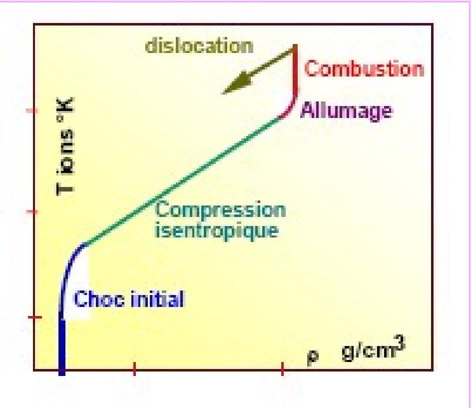

Laser-driven inertial fusion consists of four main stages

- launch of the first shock: preparation of the shell
- quasi-isentropic shell compression and adiabatic heating
- fuel ignition at the moment of stagnation
- combustion of the cold fuel in the shell
- expansion of the shell remnants and reaction products

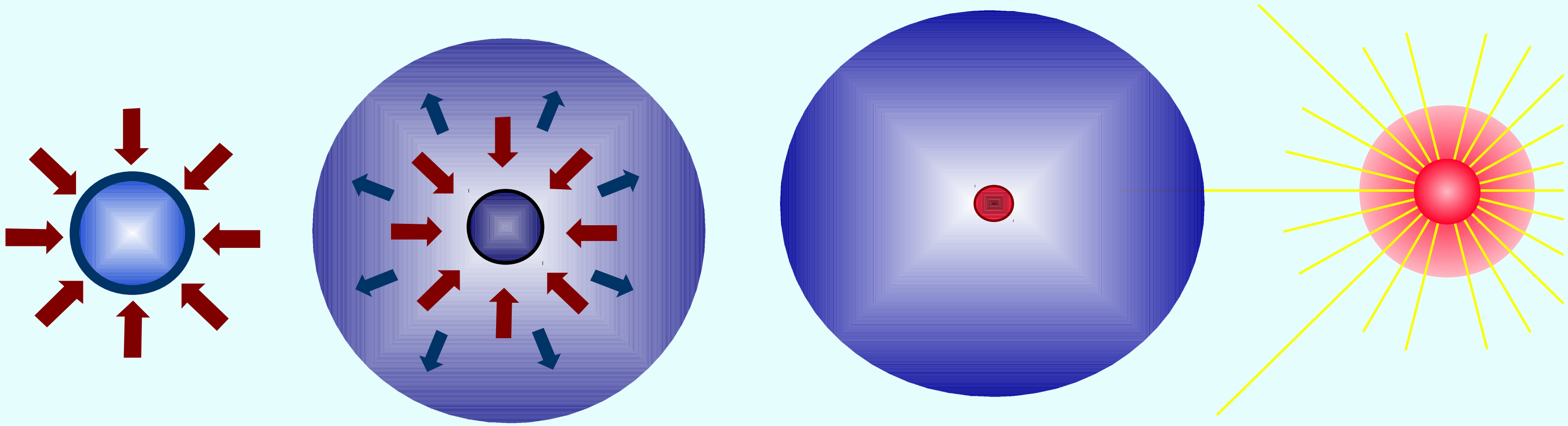

Laser irradiation of a spherical shell filled DT fuel and plasma ablation

Expansion of outer plasma, acceleration and compression of inner shell of DT

Shell stagnation and ignition of a central hot spot
ρ ≈ 400 g/cc T ≈ 10 keV

Fuel combustion
~ 100 ps
10 – 100 MJ
Energy recuperation

Ignition conditions

Ignition conditions (Lawson criterion) take a specific form for the ICF due to the finite life time of the hot spot and the heterogeneous structure of the fuel

$$t_{\mathrm{ign}} \approx R_{\mathrm{hs}}/c_{\mathrm{s}} = 10\,\mathrm{ps} \qquad T_{\mathrm{DT}} \approx 10\,\mathrm{keV} \qquad \rho_{\mathrm{hs}} R_{\mathrm{hs}} \geq 0.2\,\mathrm{g/cm^2} \qquad \rho_{\mathrm{shell}} R_{\mathrm{shell}} \geq 3\,\mathrm{g/cm^2}$$

for ρ_{shell} = 300 g/cc ρ_{hs} = 100 g/cc M_{DT} = 1 mg R_{shell} = 100 μm E_{DT} = 100 MJ

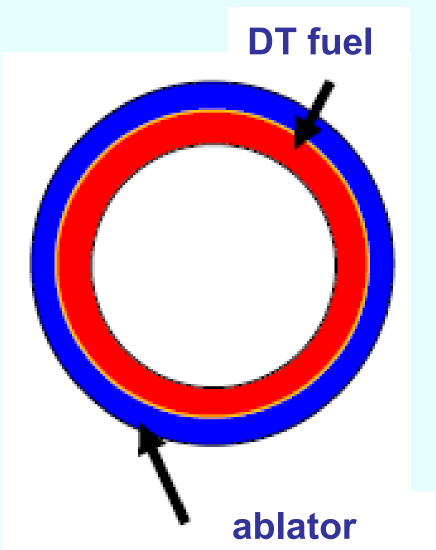

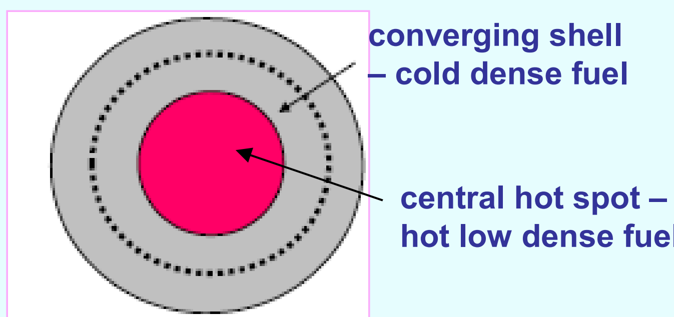

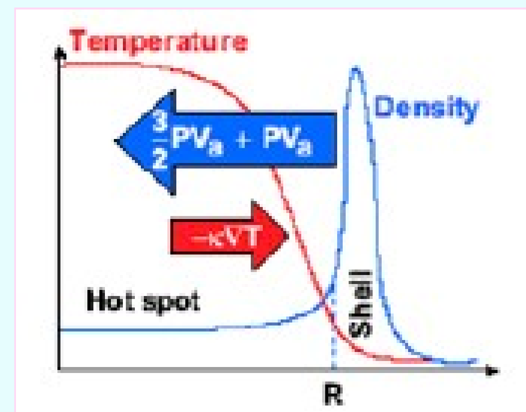

Targets are designed to burn about 30% of the fuel

Drivers for the inertial fusion

Several approaches are now under development for the ICF:

- central hot spot ignition
  - direct drive laser fusion
  - shock ignition
  - indirect drive laser fusion
  - heavy ion fusion
- ex-central hot spot ignition
  - fast ignition with electrons (with and w/out cone)
  - fast ignition with ions
  - impact ignition

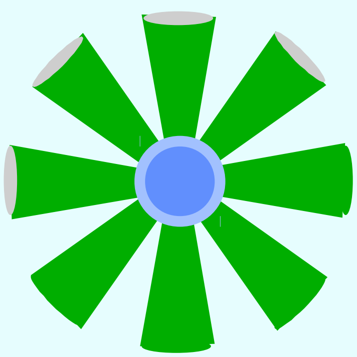

direct drive with lasers

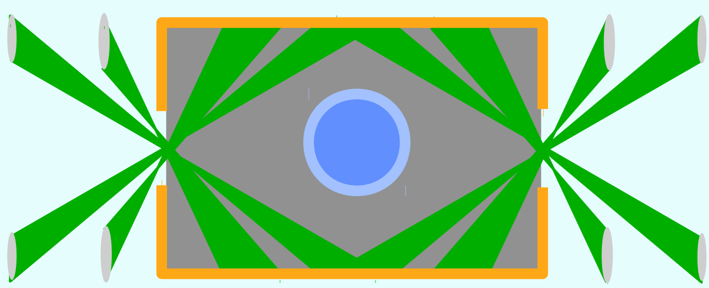

indirect drive by X-rays

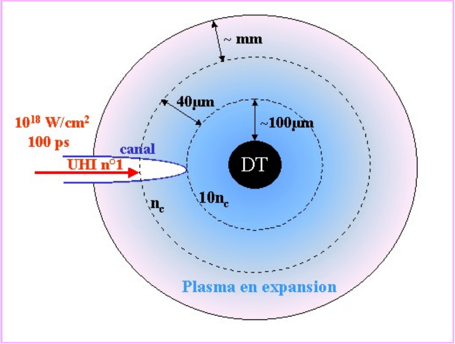

fast ignition with PW pulse

Indirect drive ICF: breakeven demonstration

Indirect drive is the most conservative approach:

- low risk of hydrodynamic instabilities
- low risk of parametric instabilities
- but complicated target design
- low efficiency
- low gain

It is chosen for current generation of the ICF installations: NIF and LMJ

talk of Catherine Cherfils-Clérouin

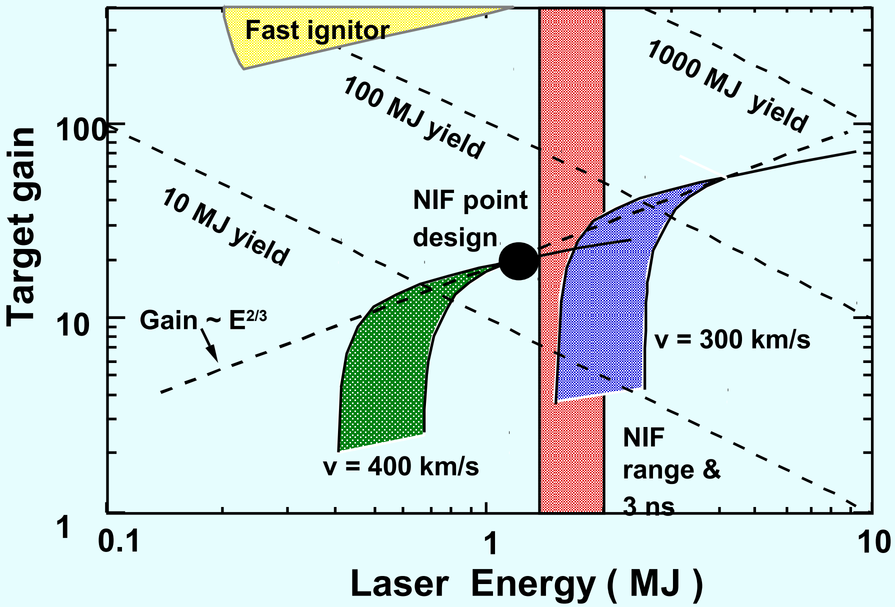

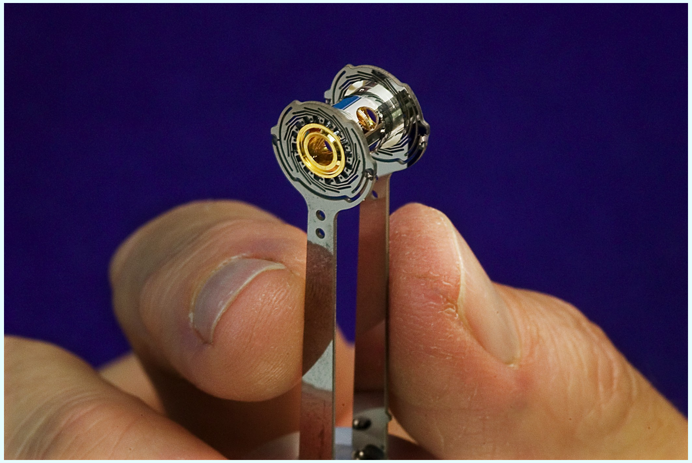

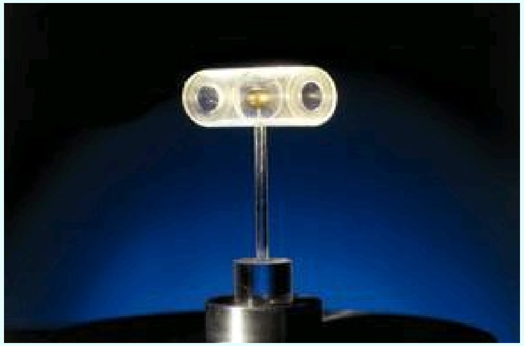

Physical processes involved in the ICF

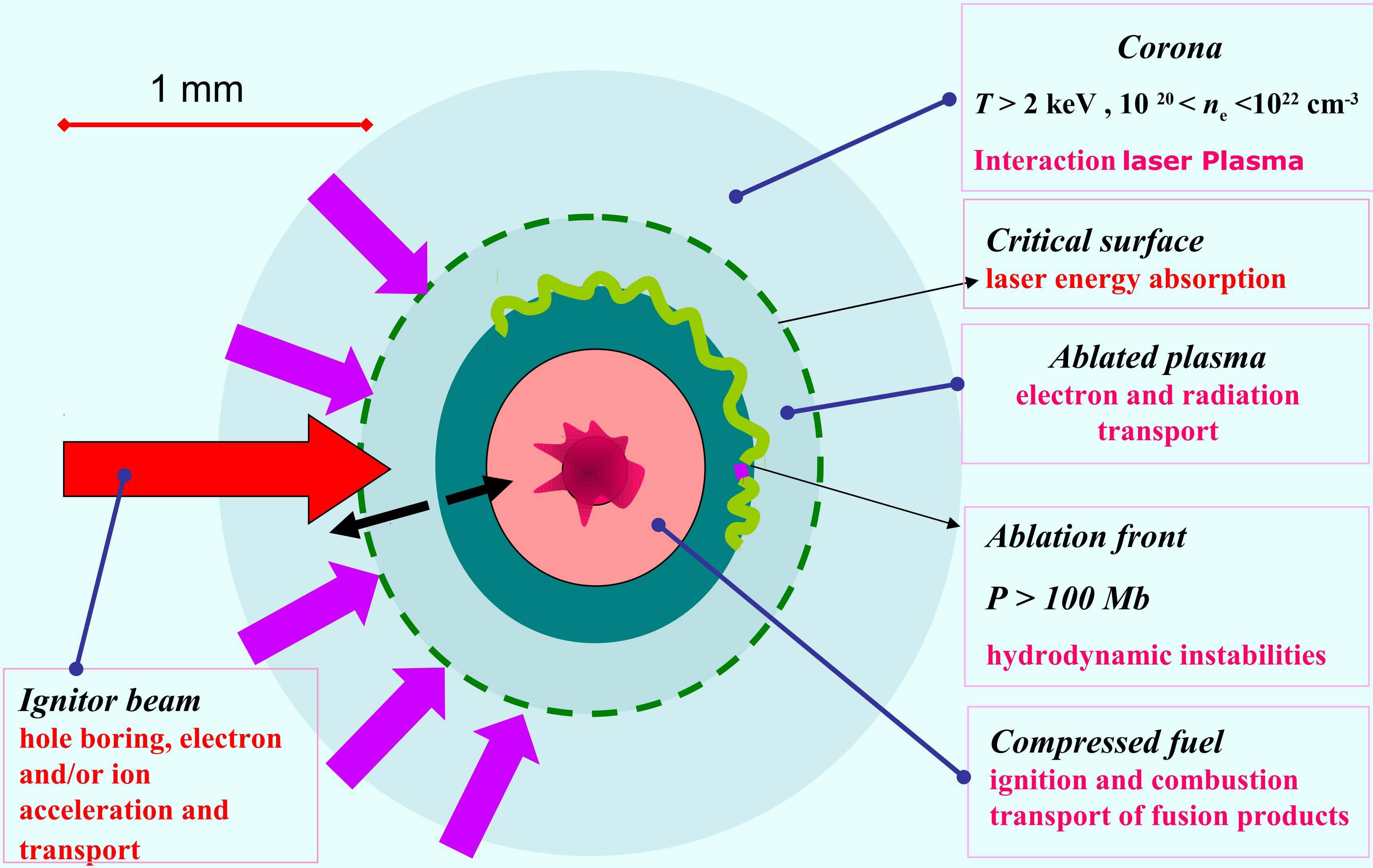

The Maxwell-Fokker-Planck-Landau model

•Fixed Ions: *1st* picoseconds of interaction: $\frac{m_e}{m_i} << 1$

•Non relativistic regime: $\frac{v_{th}}{c} << 1$ $\quad v_{th} = \sqrt{\frac{k_B T_e}{m_e}}$

$$\frac{\partial f_e}{\partial t} + \nabla_x \cdot (\mathbf{v} f_e) + \nabla_v \cdot \left(\frac{q_e}{m_e} (\mathbf{E} + \mathbf{v} \times \mathbf{B}) f_e \right) = C_{ee}(f_e, f_e) + C_{ei}(f_e)$$

$$\frac{\partial \mathbf{E}}{\partial t} - c^2 \nabla_x \times \mathbf{B} = -\frac{J}{\epsilon_0}$$

$$\frac{\partial \mathbf{B}}{\partial t} + \nabla_x \times \mathbf{E} = 0$$

$$J = \int_{\mathbb{R}^3} f_e(\mathbf{x}, \mathbf{v}, t) d\mathbf{v}$$

Gauss equations are satisfied at any time
provided they are satisfied at initial time.

$$C_{ee} = \frac{e^4 \Lambda}{8\pi \epsilon_0^2 m_e^2} \nabla_v \cdot \int_{\mathbb{R}^3} \Phi(\mathbf{v} - \mathbf{v}') \left[f_e(\mathbf{v}') \nabla_v f_e(\mathbf{v}) - f_e(\mathbf{v}) \nabla_{v'} f_e(\mathbf{v}') \right] \mathbf{dv}'$$

$$C_{ei} = \frac{Z n_0 e^4 \Lambda}{8\pi \epsilon_0^2 m_e^2} \nabla_v \cdot \left[\Phi(\mathbf{v}) \nabla_v f_e(\mathbf{v}) \right]$$

, where: $\Phi(\mathbf{u}) = \frac{|\mathbf{u}|^2 Id - \mathbf{u} \otimes \mathbf{u}}{|\mathbf{u}|^3}$

Numerical schemes validation on the full collisional model *

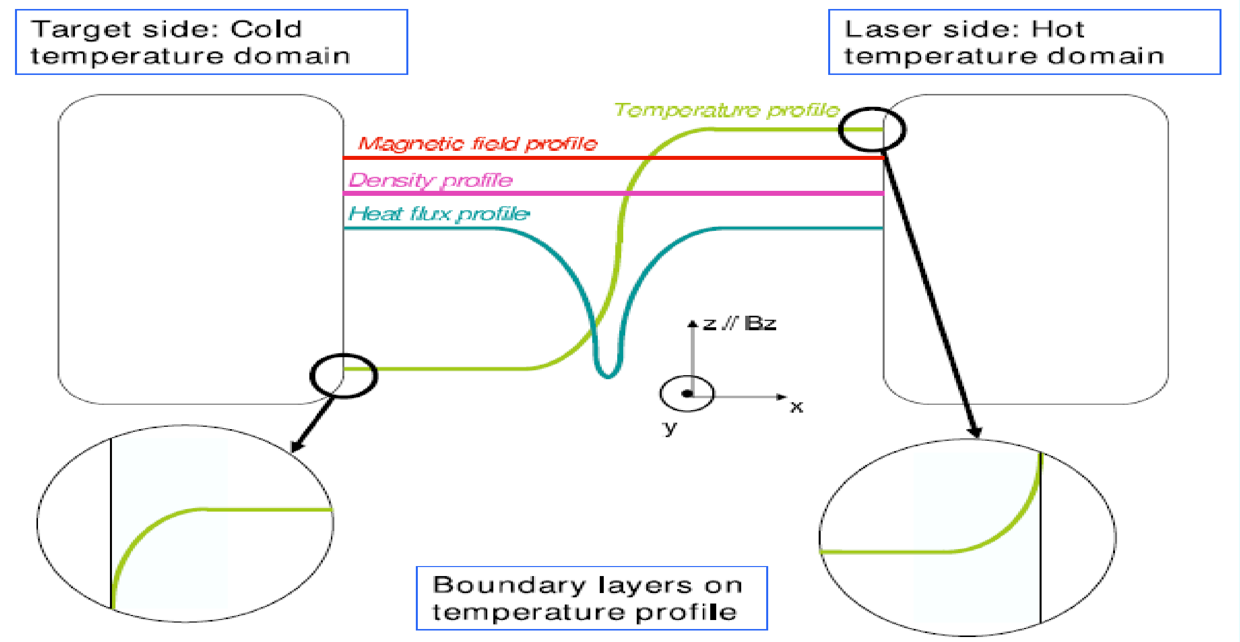

Analytical solution in the local regime:

$$Kn = \frac{\lambda_{ei}}{\lambda_{pert}} < 10^{-3}$$

$$q_x = -\frac{5}{2} T_e n_e^{-1} j_x - \chi T_e B_z^{-1} \nabla_x T_e \kappa_\perp^c - T_e \left(\beta_\perp^c j_x - \beta_\wedge^c j_y \right)$$

$$q_y = -\frac{5}{2} T_e n_e^{-1} j_y - \chi T_e B_z^{-1} \nabla_x T_e \kappa_\wedge^c - T_e \left(\beta_\perp^c j_y + \beta_\wedge^c j_x \right)$$

$$E_x = n_e{}^{-1} j_y B_z - n_e^{-1} \nabla_x p - \nabla_x T_e \beta_\perp^c + n_e{}^{-1} B_z \chi^{-1} (\alpha_\perp^c j_x + \alpha_\wedge^c j_y)$$

$$E_y = -n_e{}^{-1} j_x B_z - \nabla_x T_e \beta_\wedge^c + n_e{}^{-1} B_z \chi^{-1} (\alpha_\perp^c j_y - \alpha_\wedge^c j_x)$$

* CEA/CCRT-PLATINE facilities

Numerical schemes validation on the full model. Spitzer-Härm regime (i)

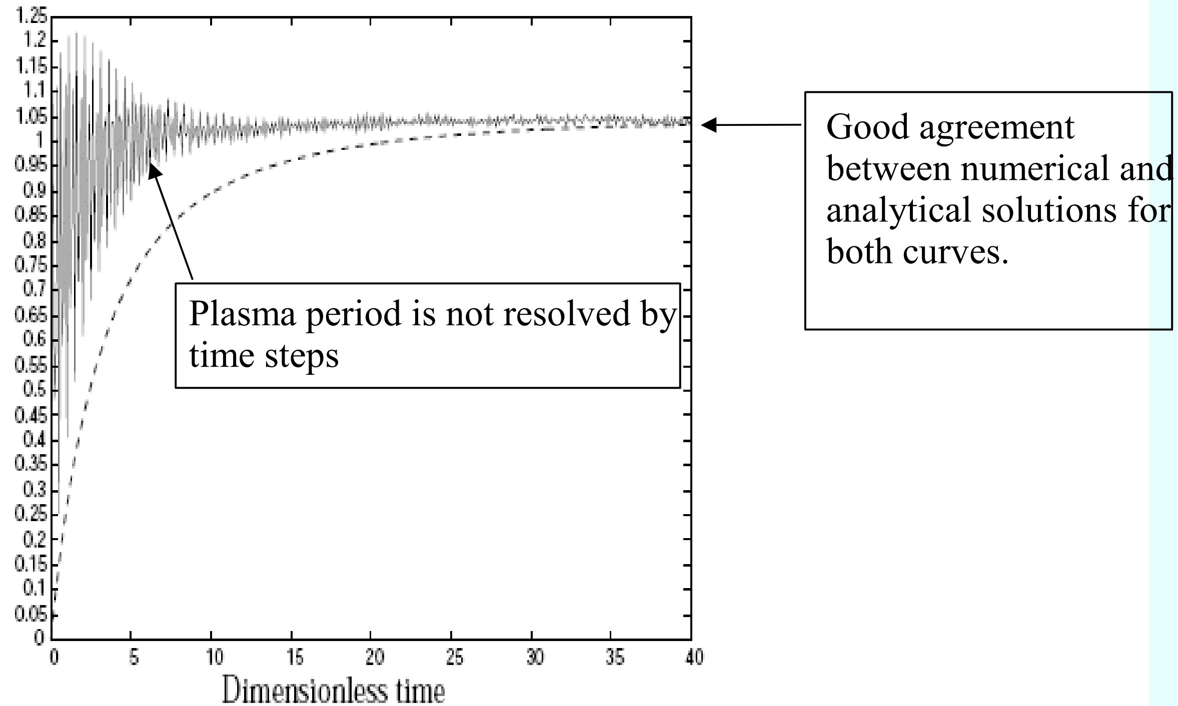

Figure : *Longitudinal (along the temperature gradient) ratios* $\frac{max_x(Q_{FP})}{max_x(Q_{BR})}$ *(dashed curve) and* $\frac{max_x(E_{FP})}{max_x(E_{BR})}$ *(oscillating curve) are shown against the dimensionless time. Dimensionless magnetic field is* $B_z = 0.001$.

126 space points, 42 processors, 24 hours simulation

Numerical schemes validation on the full model. Braginskii regime (ii)

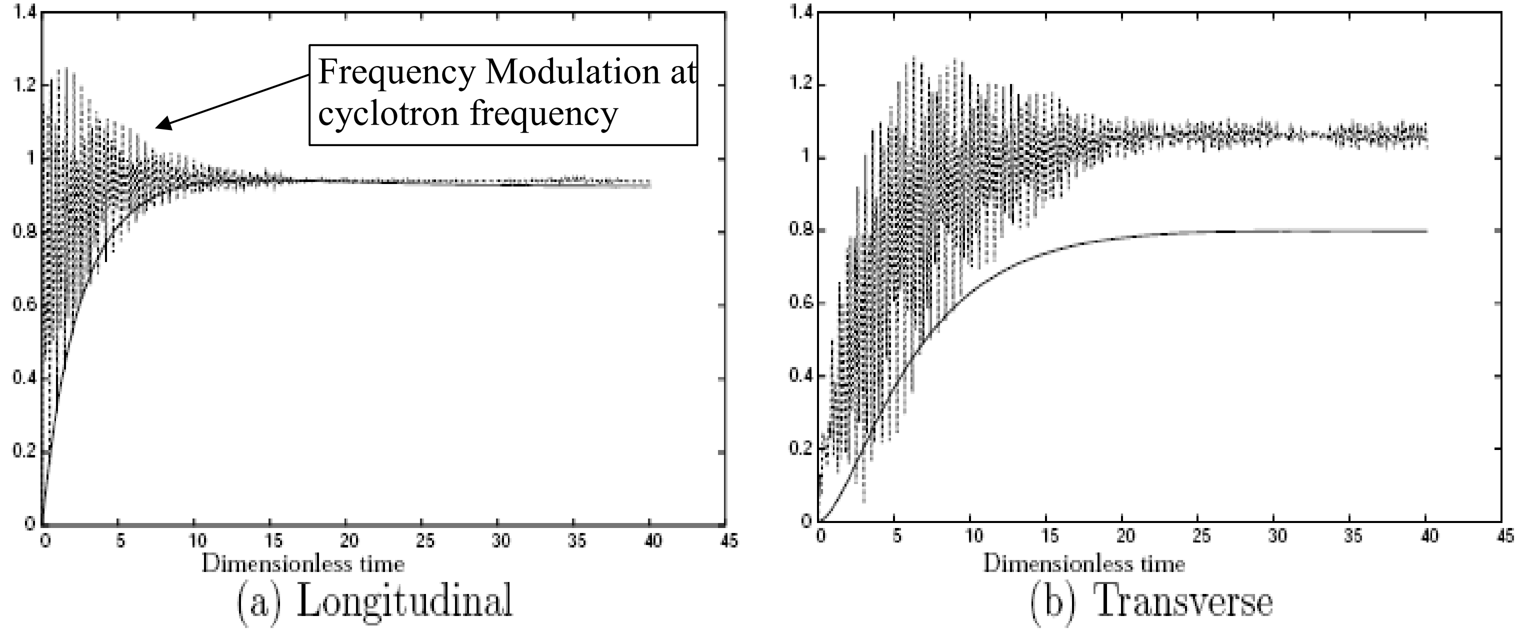

Figure : *Ratios* $\frac{max_x(Q_{FP})}{max_x(Q_{BR})}$ *(curve in bold) and* $\frac{max_x(E_{FP})}{max_x(E_{BR})}$ *(dashed curve) are shown against the dimensionless time.*

Dimensionless magnetic field is $B_z = 0.1$.

126 points, 42 proc. Simulation is Larmor radius independent: 1260 points, 420 proc. 24 hours.

Numerical schemes validation on the full model. Braginskii regime (iii)

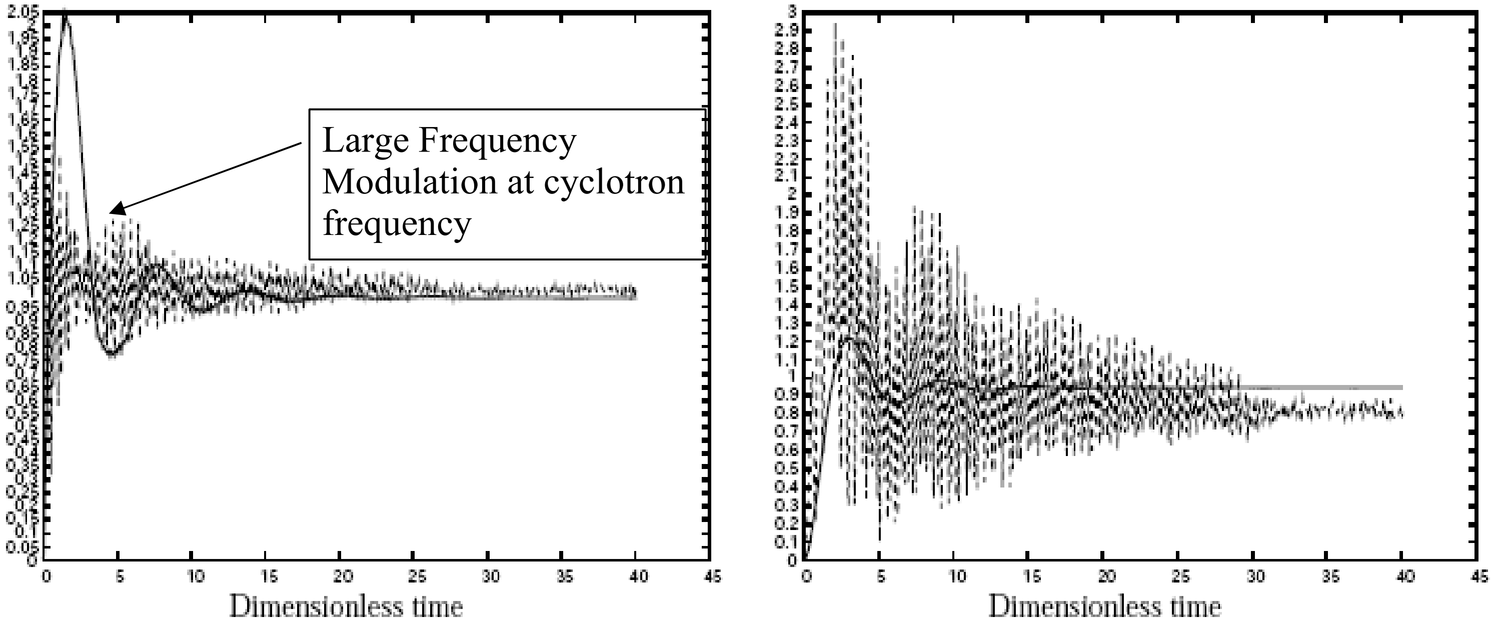

(a) Longitudinal (b) Transverse

Figure 9: *Ratios* $\frac{max_x(Q_{FP})}{max_x(Q_{BR})}$ *(curve in bold) and* $\frac{max_x(E_{FP})}{max_x(E_{BR})}$ *(dashed curve) are shown against the dimensionless time.*

Dimensionless magnetic field is $B_z = 1$.

126 points, 42 proc. Simulation is Larmor radius independent: 6300 points, 2100 proc. 24 hours

Numerical schemes validation on the full model. 2D nonlocal, magnetized regime (v)

Temperature relaxation of a Laser Speckle with cylindrical symmetry:
Initial zero fields; Initial constant density, remaining constant over time;

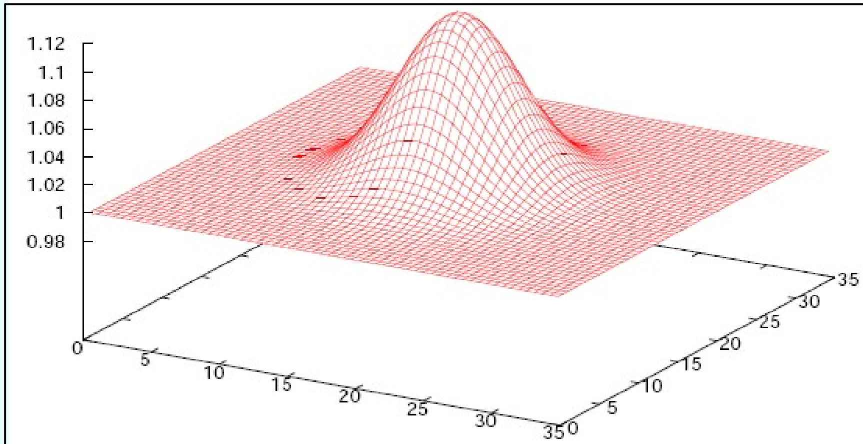

Figure:Temperature initial profile

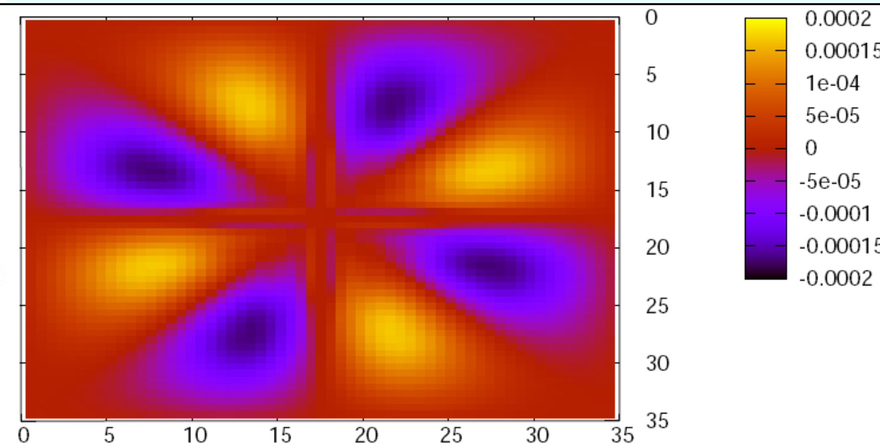

Figure: Nonlocal generation of B field after ~1ps

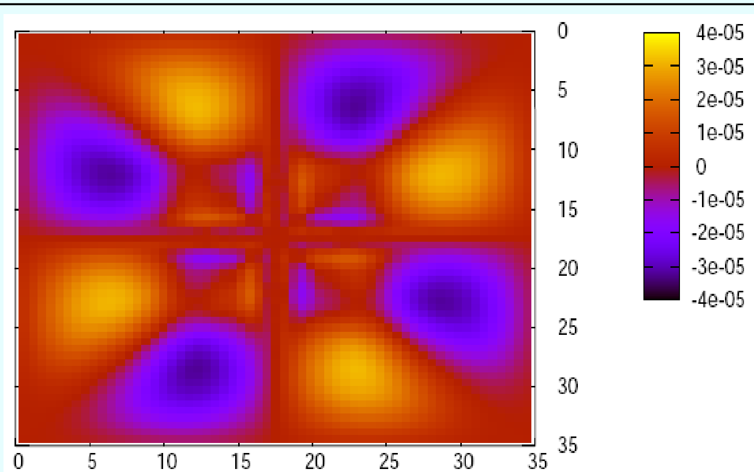

Figure:Cross gradient of high order moments

Structure is expained by the approximated formula [Kingham,Bell,PRL,2002]:

$$\frac{\partial B(x,t)}{\partial t} \propto \nabla_x \int_{\mathbb{R}^3} f_e(\mathbf{x},\mathbf{v},t)\mathbf{v}^3 d\mathbf{v} \times \nabla_x \int_{\mathbb{R}^3} f_e(\mathbf{x},\mathbf{v},t)\mathbf{v}^5 d\mathbf{v}$$

400 proc. 12 hours simulation

Introduction modèles réduits

Contexte

Nouveau modèle de transport pour les électrons.

Comment

Fermeture des équations de transport en intégrant sur les directions de propagation et en gardant l'énergie des particules comme une variable : on passe de 6 à 4 dimensions.

Propriétés du modèle

- Exact pour les faisceaux et en régime isotrope,
- résultats très proche du modèle microscopique initial,
- faible coût de calcul.

Avantages

Comparaison calcul cinétique FKP/M1

Cinétique : beaucoup de ressources $\longleftrightarrow$ M1 : faible temps calcul

exemple : $32^3 \times 100^2 \quad \longrightarrow \quad 4 \times 32 \times 100^2$

$\div 256$

Comparaison P1/M1

$\rightsquigarrow$ P1

$f(|v|) = \alpha_0(|v|) + \mu\alpha_1(|v|)\ (\mu = \cos(\theta))$

$f_0 = \frac{1}{2}\int_{-1}^{1} f d\mu$ and $f_1 = \frac{1}{2}\int_{-1}^{1} f \mu d\mu \ \Rightarrow\ f(|v|) = f_0 + 3\mu f_1$

$$\boxed{f \geq 0 \ \Leftrightarrow \frac{f_1}{f_0} \leq \frac{1}{3}}$$

$\rightsquigarrow$ M1

$$\boxed{f(|v|) = exp(\alpha_0(|v|) + \alpha_1(|v|)\mu) \geq 0}$$

Modèle M_1

Principe de la fermeture angulaire

Réduction du coût basé sur un principe de minimisation d'entropie pour la distribution angulaire des particules

Trois premiers moments en angles

S_2 est la sphère unité, $\Omega = v/|v|$ est la direction de propagation des particules. Dans ce cas, si nous posons $\zeta = |v|$, on peut définir les trois premiers moments en angle,

- $f_0(\zeta) = \zeta^2 \int_{S_2} f(v)\, d\overrightarrow{\Omega}$: masse
- $f_1(\zeta) = \zeta^2 \int_{S_2} \overrightarrow{\Omega} f(v)\, d\overrightarrow{\Omega}$: quantité de mouvement
- $f_2(\zeta) = \zeta^2 \int_{S_2} \overrightarrow{\Omega} \otimes \overrightarrow{\Omega} f(v)\, d\overrightarrow{\Omega}$: énergie

Electron Transfer Equation

Only absorption for simplicity

$$\partial_t f(t,x,v) + v.\nabla_x f(t,x,v) = -\sigma_a(x) f(t,x,v),$$

where $f = f(t,x,v)$ is the distribution function of electrons, $\Omega \in S_2$ is the propagation direction and $\zeta = |v| \geq 0$ is the energy of particles.

Problem

equation too expensive (6 dimensions), need to rescale the problem to obtain macroscopic model.

Minimun entropy principle (Levermore, Minerbo)

$$f = \rho_0(\zeta) \exp(-\Omega \cdot a_1(\zeta)),$$

where ρ_0 is a non negative scalar ($\rho_0 \geq 0$), and a_1 is a three component real valued vector.

M_1 closure

M_1 system

$$\begin{aligned} \partial_t f_0(t,x,\zeta) &+ \nabla_x \cdot (\zeta f_1(t,x,\zeta)) = -\sigma_a(x) f_0(t,x,\zeta), \\ \partial_t f_1(t,x,\zeta) &+ \nabla_x \cdot (\zeta f_2(t,x,\zeta)) = -\sigma_a(x) f_1(t,x,\zeta), \end{aligned}$$

where $f_0(\zeta) = \zeta^2 \int_{S_2} f(v)\, d\Omega$ and $f_1(\zeta) = \zeta^2 \int_{S_2} \Omega f(v)\, d\Omega$. The closure is given by $f_2(\zeta) = \zeta^2 \int_{S_2} \Omega \otimes \Omega f(v)\, d\Omega$.
The normalized flux is written as $\alpha = \frac{f_1}{f_0}$.

Physical constraints

The moments f_0 and f_1 must verify that $f_0 \geq 0$ and that $|\alpha| \leq 1$ (flux limitation).

M_1 closure

χ factor

$$\chi \approx \frac{a_6\,\alpha^6 + a_4\,\alpha^4 + a_2\,\alpha^2 + a_0}{\alpha^4 + b_2\,\alpha^2 + b_0},$$

$$\begin{aligned} a_0 &= 0.7620, & b_0 &= 2.2862 \\ a_2 &= 0.2191, & b_2 &= -2.107, \\ a_4 &= -0.2597, & & \\ a_6 &= 0.4571. & & \end{aligned}$$

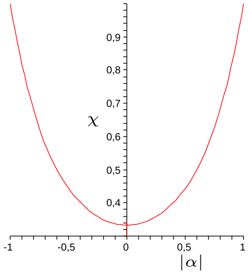

The electron pressure is given by

$$f_2 = f_0 \left(\frac{1-\chi(|\alpha|)}{2} I + \frac{3\chi(|\alpha|)-1}{2} \frac{f_1}{|f_1|} \otimes \frac{f_1}{|f_1|} \right),$$

where χ factor is given by a rational approximation.

Properties of the M_1 system

The electron moment model M_1 has the following properties

1. the electron energy f_0 remains positive : $f_0 \geq 0$,
2. the normalized flux is limited : $|\alpha| \leq 1$,
3. the system is hyperbolic,
4. the M_1 system recovers the equilibrium diffusion regime as relaxation limit for large absorption coefficient.

Numerical approximation must verify

1. the electron energy $f_{0,i}^n$ remains positive,
2. the normalized flux is limited : $|\alpha_i^n| \leq 1$,

Numerical approximation of M_1 system

Approximate Riemann solver HLLC in collaboration with C. Berthon

- two states solver to take into account the material speed λ_0,
- based on reformulation (B. Després) of the variables $f_1 = \beta(f_0 + \Pi)$, $f_2 = \beta \otimes f_1 + \Pi Id$ where β is the material speed and Π the interface pressure,
- the wave speed β is solution of a quadratic equation,
- good estimation of the speed of left and right extremal waves of Riemann problem.

High order extension

- MUSCL approach with slope limitation with order 2 or 4,
- Extra limitation needed to ensure flux limitation (From C. Berthon work on Euler Equation).

Landau effect

M_1 equation for electrostatic case

$$\partial_t f_0 + \partial_x(\zeta f_1) - \partial_\zeta(E f_1) = 0,$$
$$\partial_t f_1 + \partial_x(\zeta f_2) - \partial_\zeta(E f_2) + \frac{(f_0 - f_2)E}{\zeta} = 0,$$
$$\partial_x E = 1 - \int_0^\infty f_0(\zeta) d\zeta,$$

Dispersion relation for M_1

$$\omega = \sqrt{1 + 2.916k^2} - i\left(\frac{0.19}{k^3} + \frac{0.085}{k^5}\right)\exp\left(-\frac{0.88}{k^2}\right)$$

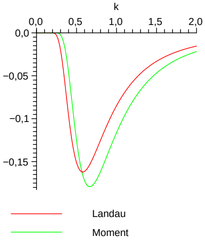

Landau effect
Validation for $k = 0.42$

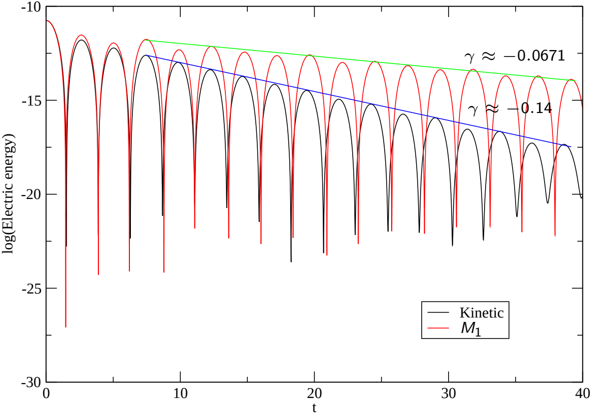

Dispersion analysis values

$\gamma_{M_1} \approx -0.062$, $\gamma_{Landau} \approx -0.12$

Two beams instability

Microscopic instabilities

- two-stream,
- filamentation,
- Weibel ...

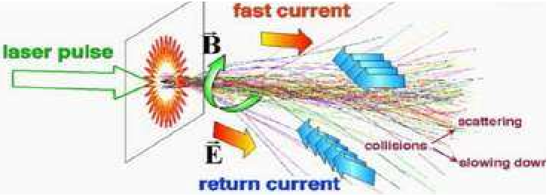

Initial conditions

$$
\begin{aligned}
f(0,x,v) &= \frac{1}{2}(1 + A\cos(kx))\exp(-(v - v_d)^2) \\
&+ \frac{1}{2}(1 - A\cos(kx))\exp(-(v + v_d)^2) \\
E(0,x) &= 0
\end{aligned}
$$

Two beams instability

Validation for $k = 0.25$ and $v_d = 4$

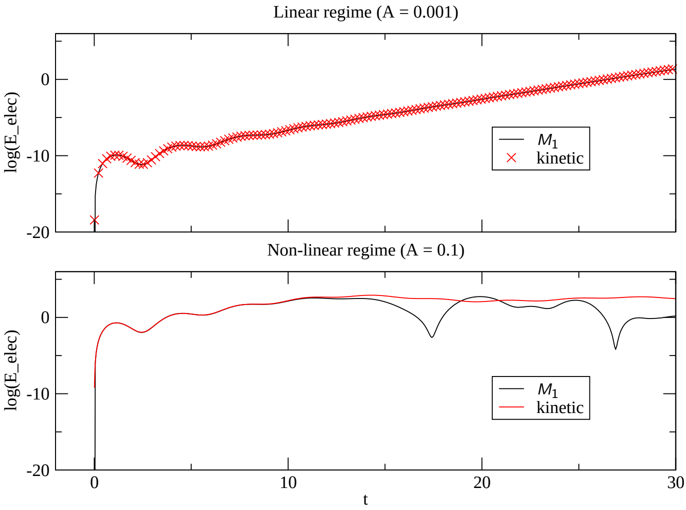

Validation of M_1 model in real radiotherapy application

Photon electron interaction

- Compton (inelastic scattering)
- relativistic electrons (Mev)

Electron-atom interaction

- Moller (inelastic) scattering : ionization, electron cascades and energy deposition
- Mott (elastic) scattering

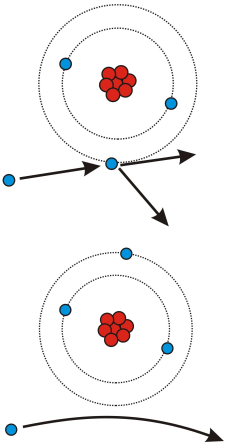

Radiotherapy application : kinetic

$$
\begin{aligned}
\frac{1}{|v(\epsilon)|} \quad & \frac{\partial \Psi}{\partial t}(t,x,\epsilon,\Omega) + \Omega \cdot \nabla \Psi(t,x,\epsilon,\Omega) = \\
& \rho_e(t,x) \int_{\epsilon_b}^{\infty} \int_{S_{2,1/4}} \tilde{\sigma}_M(\epsilon',\epsilon,\Omega'\cdot\Omega)\ \Psi(t,x,\epsilon',\Omega') d\Omega' d\epsilon' \\
+ \quad & \rho_e(t,x) \int_{\epsilon_b}^{\infty} \int_{S_{2,2/4}} \tilde{\sigma}_{M,\delta}(\epsilon',\epsilon,\Omega'\cdot\Omega)\ \Psi(t,x,\epsilon',\Omega') d\Omega' d\epsilon' \\
+ \quad & \rho_c(t,x) \int_{S_2} \sigma_{Mott}(x,\epsilon,\Omega'\cdot\Omega)\ \Psi(t,x,\epsilon,\Omega') d\Omega' \\
- \quad & \rho_e(t,x)\ \sigma_{M,tot}(\epsilon)\ \Psi(t,x,\epsilon,\Omega) \\
- \quad & \rho_c(t,x)\ \sigma_{Mott,tot}(x,\epsilon)\ \Psi(t,x,\epsilon,\Omega),
\end{aligned}
$$

where $\Psi = |v(\epsilon)| f$, ϵ is the energy of particles, ρ_e is the electron medium density and ρ_c is the core medium density. σ are very peaked.

Radiotherapy application : M_1

Equations

$$\begin{aligned}
\frac{1}{|v(\epsilon)|}\frac{\partial \Psi_0}{\partial t}(t,x,\epsilon) &+ \nabla\cdot\Psi_1(r,\epsilon,t) = \frac{\partial}{\partial \epsilon}\left[S_M(x,\epsilon)\Psi_0(t,x,\epsilon)\right],\\
\frac{1}{|v(\epsilon)|}\frac{\partial \Psi_1}{\partial t}(t,x,\epsilon) &+ \nabla\cdot\Psi_2(t,x,\epsilon) = \frac{\partial}{\partial \epsilon}\left[S_M(x,\epsilon)\Psi_1(t,x,\epsilon)\right]\\
&- 2\Psi_1(t,x,\epsilon)\left[T_{Mott}(x,\epsilon)+T_M(x,\epsilon)\right],
\end{aligned}$$

where $\Psi_0 = \int_{S_2}\Psi d\Omega, \Psi_1 = \int_{S_2}\Omega\Psi d\Omega, \Psi_2 = \int_{S_2}\Omega\otimes\Omega\Psi d\Omega.$

Absorbed dose calculation

$$D(t,x) = \frac{mc^2}{\rho_c(x)}\int_{\epsilon_b}^{\infty} S_M(x,\epsilon)\Psi_0(t,x,\epsilon)d\epsilon,$$

where $S_M(x,\epsilon)$ is the stopping power of electrons (from Pomraming 1992).

Validation

Comparaison avec le code Monte-Carlo PENELOPE

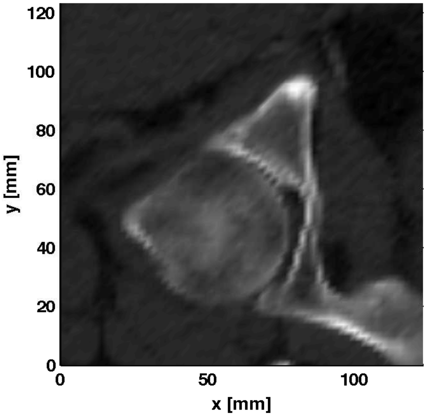

64×64 cellules en x, y, ϵ, 3 faisceaux de 10 Mev.

Comparaison avec le code Monte-Carlo PENELOPE

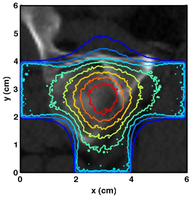

(a) Solution Monte Carlo.

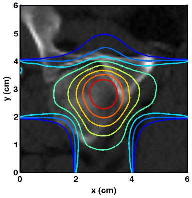

(b) Solution M_1.

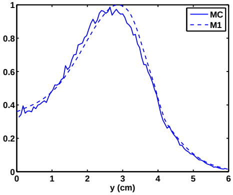

(c) Coupe sur $x = 3$ cm.

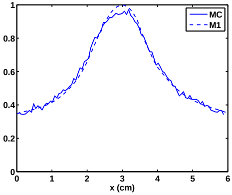

(d) Coupe sur $y = 3$ cm.

15 s sur 8 processeurs en OPENMP pour M_1 et 72h pour PENELOPE.

Autre cas : colonne vertébrale

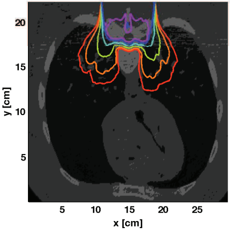

(b) Minimum entropy solution.

Figure 4. Isodose curves for electron beam on vertebral column. Normalised by D_{max}, they are shown as 5% red, 10% orange, 25% yellow, 50% light blue, 70% dark blue, 80% violet.

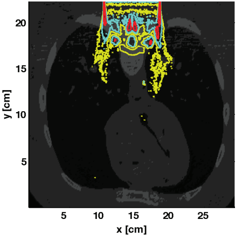

Figure 5. Contour plot of the dose differences between the M1 model and PENELOPE, scaled by the maximum dose (2% difference shown in yellow, 5% difference cyan, 10% difference red).

Faisceau de 15 Mev.